Science & Technology Development Journal 2026, 29(1):3936-3943

Open Access Full Text Article

Research Article

Antibacterial activity and burn wound healing properties of biosynthesized silver nanoparticles using *Mentha aquatica* L. var. *aquatica* leaf extract

Le Thi Anh Tu[1,*], Le Huu Trong[2]

ABSTRACT

Introduction: *Mentha aquatica* L. var. *aquatica* is a commonly used herb with medicinal properties. Phytochemicals in the leaf extract act as reducing and stabilizing agents during the biosynthesis of silver nanoparticles (SNPs). The bactericidal and wound healing properties of SNPs biosynthesized from *M. aquatica* L. var. *aquatica* leaf extract remain largely unexplored. This study therefore aimed to optimize SNP biosynthesis from *M. aquatica* L. var. *aquatica* leaf extract and investigate its antimicrobial properties against *S. aureus* (gram positive) and *P. aeruginosa* (gram negative) and potential applications in wound care.

Methods: SNPs were synthesized using *M. aquatica* L. var. *aquatica* leaf extract; $AgNO_3$ concentration, amount of initial leaf extract, and reaction time were analyzed to evaluate the efficiency of biosynthesis. SNPs were characterized through UV–Vis absorption, dynamic light scattering, scanning electron microscopy, and transmission electron microscopy. The functional groups of the leaf extract and SNPs were investigated using Fourier transform infrared spectros-copy (FTIR). Further analyses using the well diffusion method and burn wound contraction were performed to investigate the antibacterial activity and wound healing properties of SNPs in mice.

Results: Optimum SNP synthesis was attained with 5 mM $AgNO_3$, 40 mg/ml leaf extract, and a reaction time of 1 h. FTIR analysis confirmed the involvement of phytochemicals in SNP syn-thesis. SNPs had an average size of 67.05 nm with an irregular spherical shape. SNPs inhibited *P. aeruginosa* (ATCC 15442) and *S. aureus* (ATCC 6538); the bactericidal effects were greater on *P. aeruginosa* than *S. aureus*. SNP dressings accelerated the wound healing process without causing weight gain in mice.

Conclusions: SNPs biosynthesized from *M. aquatica* L. var. *aquatica* leaf extract inhibited *P. aeruginosa* and *S. aureus*. Dressings containing 10% SNPs accelerated wound healing in mice. SNPs could potentially be used as an antibacterial agent to promote wound healing.

Key words: Bactericidal activity, well diffusion assay, P. aeruginosa ATCC 15442, S. aureus ATCC 6538, SNPs

[1]*Biology Department, Dalat University, Dalat, Lamdong, Vietnam*

[2]*Nguyen Binh Khiem High School, Ba Ria, Ba Ria Vung Tau, Vietnam*

Correspondence

Le Thi Anh Tu, Biology Department, Dalat University, Dalat, Lamdong, Vietnam

Email: tulta@dlu.edu.vn

History

- Received: 13-11-2024
- Revised: 09-08-2025
- Accepted: 26-10-2025
- Published Online: 21-01-2026

DOI :

https://doi.org/10.32508/stdjet.v29i1.4392

INTRODUCTION

Nanotechnology has revolutionized industries such as food packaging, animal husbandry, electronics, agriculture, medicine, and healthcare[1]. Nanomaterials are characterized by their unique properties, with sizes ranging from 1–100 nm. The large surface area to surface volume ratio and optical, magnetic, chemical, and mechanical properties associated with their size have made nanomaterials candidates for novel applications in the biomedical field as antibiotics, antioxidants, and anticancer agents[2]. Cancer therapy, bioimaging, and designing are well-known applications. Expectedly, biotechnology and nanotechnology have been increasingly integrated to generate eco-friendly biosynthesized nanomaterials[3].

There are various physical, chemical, biological, and hybrid methods through which nanoparticles are synthesized. Chemical and physical methods are associated with the use of hazardous chemicals toxic to humans and ecosystems[4]. Plant-mediated synthesis of metal nanoparticles is therefore garnering attention as an alternative method, especially for healthcare-related applications. Biosynthesis is reliable, nontoxic, and eco friendly; photo-mediated synthesis is recognized as a rapid and suitable biosynthetic method for the generation of metal nanoparticles[5]. Plant extracts from leaves, seeds, barks, [A. N.6] roots, fruits, and stems have been used to synthesize nanoparticles. Plants are rich in bioactive secondary metabolites such as polysaccharides, proteins, polyphenols, flavonoids, terpenoids, tannins, alkaloids, amines, ketones, and aldehydes which act as reducing, stabilizing, and capping agents during the conversion from metal ions to metal nanoparticles[6].

Cite this article : Thi Anh Tu L, Huu Trong L. **Antibacterial activity and burn wound healing properties of biosynthesized silver nanoparticles using *Mentha aquatica* L. var. *aquatica* leaf extract**. *Sci. Tech. Dev. J.* 2026; 29(1):3936-3943.

Nanomedicine, with its broad scope, has played an important role in the global healthcare industry over the last few decades[7]. The multifunctional theranostic abilities of nanoparticles of noble metals such as gold, platinum, silver, copper, zinc, and titanium have attracted increasing attention for biomedical applications. Silver nanoparticles (SNPs) have gained significant attention among metallic nanoparticles due to their unique properties which include a low toxicity profile, antimicrobial activity, the promotion of bone healing, and the enhancement of the immunogenicity of vaccines[8,9]. Antibiotics defend against bacterial infection; however, long-term use facilitates bacterial resistance through various mechanisms[10]. Antibiotic resistance has led to the demand for new antimicrobial agents which inhibit bacterial adaptations related to antibiotic evasion. Silver is an inorganic agent able to kill various bacteria through the "oligodynamic effect"[11] with particles at the nanometer level offering greater advantages for antibacterial applications.

Many studies have been conducted on the biosynthesis of SNPs from plant extracts[12,13]; however, indigenous species with potential bactericidal and wound healing properties have not been extensively explored. Mentha is a genus of the Lamiaceae family comprising several widely used species. Extracts of this genus with significant amounts of antioxidant phenolic compounds are used as food and traditional medicine. The plant essential oils have been used to treat mild fungal and bacterial skin infections, gastrointestinal tract disorders, inflammation, and pain[14]. *Mentha aquatica* L. var. *aquatica*, a species of Mentha, is cultivated in multiple and diverse environments. This work aimed to synthesize SNPs from *M. aquatica* L. var. *aquatica* leaf extract and evaluate their antimicrobial and excision wound healing properties.

MATERIALS AND METHODS

Materials

Pseudomonas aeruginosa ATCC 15442 and *Staphylococcus aureus* ATCC 6538 were obtained from the biology department of Dalat University. Fresh *M. aquatica* L. var. *aquatica* leaves were collected from Dalat, Lamdong, Vietnam. The leaves were washed thoroughly thrice with tap water and twice with sterile water, then dried at room temperature and finely ground for SNP synthesis. The voucher specimen is available from the resources unit of the Herbarium of Dalat University, Lamdong, Vietnam. Reagents were obtained from Sigma-Aldrich.

SNP biosynthesis

The prepared *M. aquatica* L. var. *aquatica* powder was added to 200 mL distilled water and heated at 60 °C with continuous stirring for 15 min. After cooling, the mixture was filtered with Whatman No. 1 paper and the filtrate collected[15]. Various $AgNO_3$ concentrations (1, 2.5, 5 mM) were prepared to determine precursor influence on SNP formation. The efficiency of SNP biosynthesis was investigated using various initial weights of fresh leaves (2.5, 5, 10, 20, 40 mg/ml). The effect of reaction time on SNP biosynthesis under optimum conditions (including the initial weight of fresh leaves) was measured at 5 min, 30 min, 1 h, 2 h, 4 h, 8 h, 24 h, and 48 h. The reduction of silver ions to SNPs was observed by a gradual change in the color of the solution.

Characterization

A UV–Vis spectrophotometer (Specord 200 Plus, Jena, Germany) was used to investigate the optimum conditions for SNP synthesis; the absorbance spectrum of the sample was obtained in the range of 400–700 nm using aqueous leaf extract as a reference. Morphology and particle size were determined by scanning electron microscopy (SEM) on a FE-SEM S4800 HITACHI and transmission electron microscopy (TEM) on a JEOL JEM-1010 operating at 100 kV. SNP particle size distribution was determined by a particle size analyzer using dynamic light scattering (DLS) (Zetasizer Nano ZS-Zen 3600). The main functional groups of the *M. aquatica* L. var. *aquatica* leaf extract and SNPs were analyzed by Fourier transform infrared spectroscopy (FTIR) spectra using an FTIR spectrophotometer (Fourier FT-IR 4600 JASCO).

SNP antibacterial activity

Well diffusion method

Concentrations of 6.25, 12.5, 25, and 50 mg/ml biosynthesized SNPs were used to evaluate antibacterial activity against *P. aeruginosa* and *S. aureus*. The leaf extract and 0.5 mM $AgNO_3$ were used as controls. Agar wells (6 mm diameter each) were contrived in all the plates and loaded with 20 μl SNPs, leaf extract, and $AgNO_3$. All plates were seeded with pathogens. The plates were incubated at 37 °C for 24 h and the zones of inhibition were recorded.

Experimental animals

Healthy 9-week-old adult male albino mice (25 $\pm$ 2 g) were divided into eight groups, with six mice per group. The mice were maintained under a 12 h/12

h day/night cycle with water and standard chow for 7 days prior to experiments to acclimatize to the experimental environment. Mice fur was shaved, disinfection was performed with 70% ethyl alcohol, and 8-mm (diameter) full thickness excision wounds were created by grasping the marked skin with toothed forceps and dissecting using a surgical blade and scissors.

Table 1: Experimental groups

Group	Treatment	Group	Treatment
T1	No pathogen, No nano	T3	No pathogen + 10% Nano
T2	Pathogen + No Nano	T4	Pathogen + 10% Nano
T5	No pathogen + 5% Nano	T6	Pathogen + 5% Nano
T7	No pathogen + 2.5% Nano	T8	Pathogen + 2.5% Nano

P. aeruginosa, *S. aureus*, and SNPs were smeared onto the wounds at creation. Wound areas were examined on Days 2, 7, 14, and 18 following the surgical procedure and body weight was evaluated. The percentage of wound contraction was determined by the following equation:

$$Percentage\ of\ wound\ contraction = \frac{Initial\ day\ wound\ size - Specific\ day\ wound\ size}{Initial\ day\ wound\ size} \times 100$$

Statistical analysis

All experiments were conducted in triplicate. Data are represented as mean ± standard deviation from a minimum of three independent replicates. Statistical significance was evaluated by one-way ANOVA ($p \leq 0.05$).

RESULTS

SNP synthesis

The bioreduction of silver ions to SNPs was optically determined by a color change from light yellow to brown (Figure 1). SNP formation monitored by UV–Vis spectrophotometry with the wavelength of absorbance from 400–700 nm indicated that precursor ($AgNO_3$) concentration, initial weight of fresh leaves and reaction time significantly influenced nanoparticle formation.

The precursor concentrations (1, 2.5, 5 mM) used to prepare SNPs were evaluated (Figure 2). SNP formation was detected in all experiments. No peak was observed at over 450 nm. The peak positions of the surface plasmon resonances (SPRs) were 435, 439, and 445 nm in wavelength; maximum absorbances

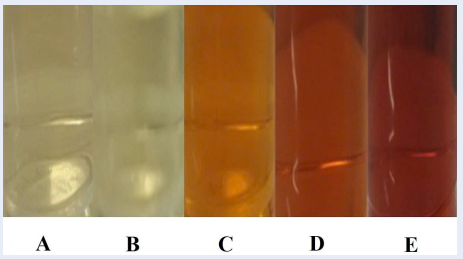

Figure 1: Silver nanoparticle color by reaction time: (A) 0 min; (B) 5 min; (C) 30 min; (D) 1 h; (E) 2 h.

were 1.464, 2.104, and 2.336 for the 1, 2.5, and 5 mM $AgNO_3$ experiments, respectively. No peak was detected with leaf extract.

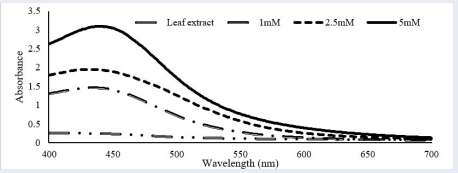

Figure 2: Effect of precursor concentration on silver nanoparticle synthesis.

Figure 3 depicts the SNP UV–Vis spectra with various initial leaf weights; sharp plasmon peaks can be observed from 434–450 nm, as expected for SNPs. The characteristic change of the mixture to a brownish color was observed in all experiments; however, the UV–Vis spectra indicated that increasing the initial leaf weight led to greater SNP formation. As the initial leaf weight increased from 2.5 to 40 mg/ml, the absorption intensity also increased. The plasmon peaks at 2.5, 5.0, 10, 20, and 40 mg/ml were 2.022, 2.337, 2.543, 2.568, and 2.798, respectively.

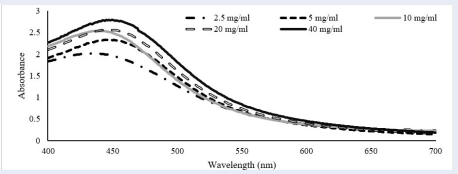

Figure 3: Effect of initial leaf weight on silver nanoparticle synthesis.

The effect of reaction time on SNP formation is shown in Figure 4 (precursor concentration and initial leaf weight at 5 mM and 40 mg/ml, respectively). SNP biosynthesis using *M. aquatica* L. var. *aquatica* leaf

extract was time dependent. No clear SPR band developed after 5 min, indicating no significant SNP formation. The band at 438 nm was observed after 30 min. The absorbance increased from 30 min to 4 h. However, when the reaction time was greater, the absorbance values were slightly reduced (8, 16, 24, and 48 h).

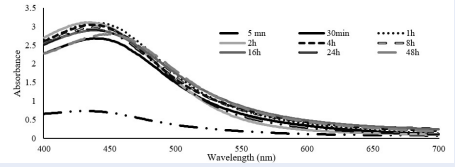

Figure 4: Effect of reaction time on silver nanoparticle synthesis.

SNP characterization

The particle size distribution of the SNP spectra obtained at different reaction times is shown in Figure 5. A wide distribution was observed. At 30 min, the average particle size was 60.88 nm. Average particle size increased with reaction time: the average particle sizes were 65.62, 67.82, 73.85, 85.07, 106.1, and 118.5 nm at 1, 2, 4, 8, 16, 24, and 48 h, respectively.

The FTIR spectrum showed some shifting of the peaks and decreasing peak intensity (Figure 6). Peak change was associated with SNP synthesis mechanisms including reduction, capping, and stabilization. Following synthesis, the peaks at 3209, 2937, 1604, and 1306 cm^{-1} shifted to 3221, 2927, 1607, and 1375 cm^{-1} and could be assigned as O–H stretching, N–H and C–H stretching, C=O, C=C, N–H stretching, and the aromatic, respectively.

The morphology of SNPs from *M. aquatica* L. var. *aquatica* leaf extract is shown in Figure 7; the particles are highly monodispersed. TEM imaging of the synthesized SNPs revealed their irregular spherical shape (Figure 7A). SEM imaging showed agglomerated SNPs with a borderline diameter and wider particle dissemination (Figure 7B).

Antibacterial activity of SNPs

SNP antibacterial activity against *P. aeruginosa* (gram negative) and *S. aureus* (gram positive) was determined using the well diffusion method (Figure 8). The aqueous leaf extract and $AgNO_3$ exhibited antibacterial activity. SNP antibacterial activity was more pronounced than that of the leaf extract and $AgNO_3$. The inhibition effect was concentration dependent. The maximum zone of inhibition at the

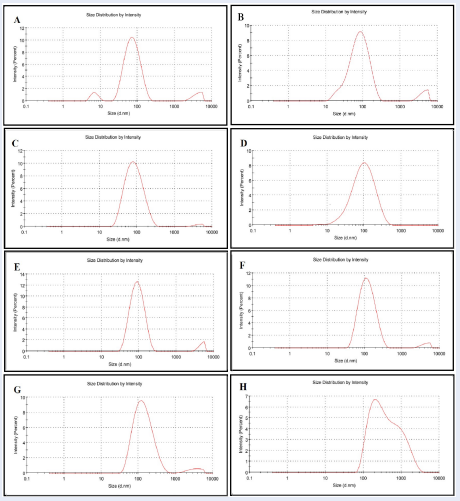

Figure 5: Particle size distribution of biosynthesized silver nanoparticles by reaction time: (A) 30 min; (B) 1 h; (C) 2 h; (D) 4 h; (E) 8 h; (F) 16 h; (G) 24 h; (H) 48 h.

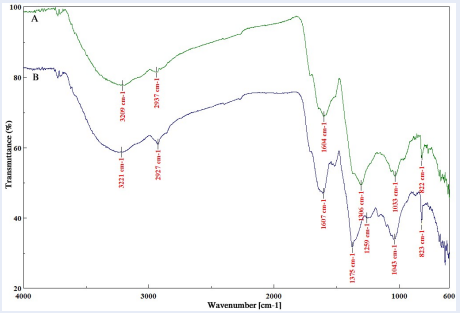

Figure 6: Fourier transform infrared spectra analysis: (A) leaf extract; (B) silver nanoparticles.

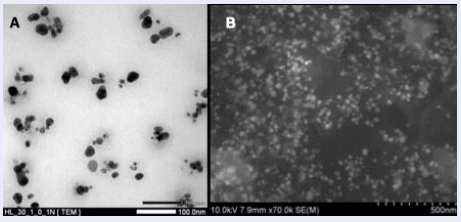

Figure 7: Morphology of biosynthesized silver nanoparticles at the 1-hour reaction time: (A) transmission electron micrograph; (B) scanning electron micrograph.

highest concentration of SNPs was 50 mg/ml against both pathogens. The inhibitive effect on *P. aeruginosa* was greater than that of *S. aureus* in a dose-dependent manner.

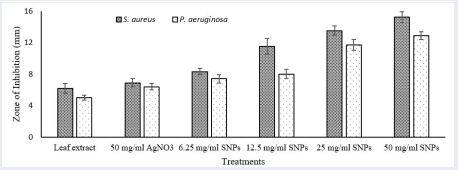

Figure 8: Silver nanoparticle (SNP) antibacterial activity against *Staphylococcus aureus* ATCC 6538 and *Pseudomonas aeruginosa* ATCC 15442.

Wound healing model

Mouse body weight variations within 18 days of different treatments are shown in Figure 9 (A and B). Body weight decreased slightly in the first 2 days, with subsequent weight regain for all treatments. The body weight of pathogen-treated mice not administered SNPs was significantly lower than other groups. The wound contraction rate of different SNP dressings used against *P. aeruginosa* and *S. aureus* was calculated as the wound size reduction 2, 7, 14, and 18 days post incision (Figure 10). After 7 days, wound healing was significantly faster in mice administered SNPs compared with pathogen-treated mice not administered SNPs and mice treated with neither pathogens nor SNPs. After 14 days, all treatments with SNPs exhibited faster wound contraction than those without SNPs (excepting treatments with 2.5% SNPs). This was the case for both *P. aeruginosa* and *S. aureus*. However, SNPs stimulated wound healing against *S. aureus* more effectively than against *P. aeruginosa*. After 14 days, the contraction rate for all treatments was 100% (excepting treatments with pathogens without SNP administration).

Re-epithelialization of wounds treated with *P. aeruginosa* and *S. aureus* (Figure 11) was complete for all dressings with SNPs after 14 days. The healed wounds of animals treated with pathogens without SNPs had thicker and darker epithelia than those treated with SNPs.

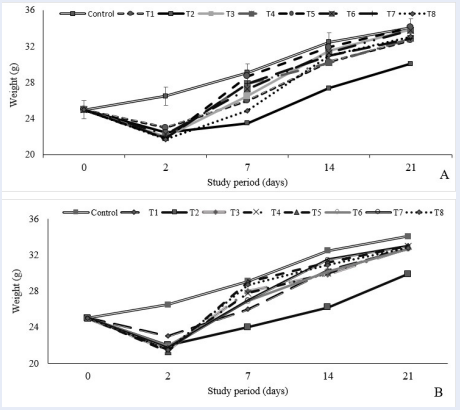

Figure 9: Body weight gain relative to weight on Day 0 in mice administered different treatments: (A) *Staphylococcus aureus* ATCC 6538; (B) *Pseudomonas aeruginosa* ATCC 15442.

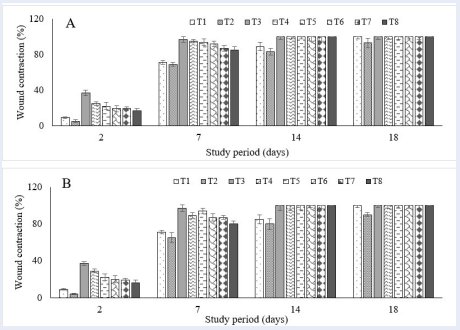

Figure 10: Wound healing as assessed by wound size reduction over time: (A) *Staphylococcus aureus* ATCC 6538; (B) *Pseudomonas aeruginosa* ATCC 15442.

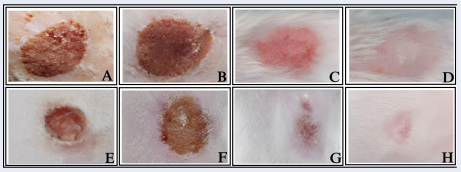

Figure 11: In vivo evaluation of the effect of silver nanoparticle (SNP) application on wound healing in mice: (A) 2 days; (B) 7 days; (C) 14 days; and (D) 18 days post incision for treatment with *Pseudomonas aeruginosa* ATCC 15442 and 10% SNPs. (E) 2 days; (F) 7 days; (G) 14 days; and (H) 18 days post incision for treatment with *Staphylococcus aureus* ATCC 6538 and 10% SNPs.

DISCUSSION

SNP biosynthesis using *M. aquatica* L. var. *aquatica* leaf extract occurs as a result of the reduction of silver ions to metallic silver by phytochemicals. SNPs exhibit a brown color in aqueous solution due to the

excitation of surface plasmonvibration [16]; this is visible evidence of SNP formation. Further evidence was obtained using UV–Vis spectrophotometry, with SPR bands between 400–500 nm. The effects of synthesis conditions including $AgNO_3$ concentration, initial leaf weight, and reaction time were evaluated to determine optimum synthesis conditions. Increasing the precursor concentration led to increased SPR intensity, indicating higher SNP yields. Plasmon peaks were observed from 435–442 nm, as expected for SNPs. Additionally, plasmon peak values (435–442 nm) suggested that SNP size did not change with increases in precursor concentration. Therefore, 5 mM of $AgNO_3$ was used for later experiments. The effect of varying the initial concentration (2.5, 5, 10, 20, 40 mg/ml) of the reducing agent (*M. aquatica* L. var. *aquatica* leaf extract) was also evaluated. An increase in the plant phytochemicals which act as reducing and capping agents, correlated with the use of more leaf extract, led to greater SNP yield [17–19].

The effect of reaction time on SNP synthesis was investigated at 5 min, 30 min, 1 h, 2 h, 4 h, 8 h, 16 h, and 24 h (Figure 4). The plasmon peak was slightly visible at 5 min. SNP formation was detected clearly at 30 min. Increased SNP formation was observed when the reaction time increased to 8 h. The absorbance intensity values slightly decreased from 16 to 24 h. SPR peak positions showed that variation in particle size at 1 to 4 h was low; however, when reaction time increased (48 h), the absorbance intensity values were lower and the plasmon peak wavelength slightly increased. Peaks with higher wavelengths indicated an increase in particle size [20,21]. Agglomeration facilitated by longer reaction times increased particle size, leading to lower absorbance intensities and higher plasmon peak values [22]. Previous studies have reported alterations in nano size with prolonged reaction times [23–25]. The FTIR spectrum corresponded to the flavonoids, steroids, tannins, alkaloids, phenolics, saccharides, and proteins in the leaf extract which facilitate SNP formation. The peaks indicated the presence of phytochemicals in the *M. aquatica* L. var. *aquatica* leaf extract, including phenolic compounds, methylene or aliphatic groups, alkenyl or aromatic compounds, fluoro compounds, and carboxylic compounds [26]. The peak shifts confirmed phytochemical involvement in SNP reduction and stabilization.

SNPs exhibited more pronounced antibacterial activity against *P. aeruginosa* and *S. aureus* in terms of inhibition zone than the leaf extract and $AgNO_3$. While *S. aureus* is a common skin pathogen, *P. aeruginosa* is representative of opportunistic pathogens with high intrinsic resistance, making it an excellent test subject for assessing a product's broad-spectrum efficacy. SNP antibacterial activity was dose dependent. These results agree with previous studies [27–29]. SNPs exhibit broad-spectrum antibacterial activity even at low concentrations not toxic to macrophages [30]. The bactericidal mechanisms of nanoparticles include the production of reactive oxygen species (ROS), compromising cell membranes, interrupting energy transduction, and inhibiting enzyme activity [31–33]. The maximum zone of inhibition was observed with 50 mg/ml SNPs for both *P. aeruginosa* and *S. aureus*. After 24 h of incubation at 37 °C, the inhibition zones against *S. aureus* were larger than those against *P. aeruginosa*. SNP bactericidal properties involve four mechanisms: (1) adhesion to the cell wall surface and membrane disruption, (2) penetration and damage to intracellular structures and biomolecules, (3) generation of ROS and free radicals, and (4) modulation of signal transduction pathways. Other studies have reported that SNP antibacterial activity is more pronounced in gram-negative than gram-positive bacteria [34]. Gram-negative bacteria have cell walls comprising an outer membrane containing lipopolysaccharide and a thin peptidoglycan layer; conversely, a thick layer of peptidoglycan, lipoteichoic acid, and teichoic acid characterize gram-positive bacteria. SNPs exhibit more pronounced bactericidal activity against gram-negative bacteria than gram-positive bacteria due to the relative abundance of negative charges on gram-negative bacteria [35]. These findings align with other studies on SNP bactericidal activity [34,36,37].

Previous studies have reported the antimicrobial properties of SNPs synthesized from *M. aquatica* L. var. *aquatica* leaf extract in vitro, but few have conducted in vivo experiments. While mouse body weight decreased in the first 2 days post incision, the weight of mice administered SNPs increased in all treatments. Body weight altered in a dose-dependent manner. On Day 7, there were no significant differences in body weight between mice treated with 10% SNP dressings and the controls, indicating that SNPs had no influence on weight gain.

The wounds treated with different SNP dressings used against *S. aureus* and *P. aeruginosa* demonstrated enhanced contraction compared with the pathogen-treated wounds without SNP application. SNPs accelerated wound healing, potentially due to pathogen inhibition and enhancement of the closure rate [38]. Other studies have reported the ability of SNPs to strengthen antioxidant activity, promote epithelialization, reduce inflammation, and improve granulation tissue formation [39,40]. After Day 18, all wounds

were closed in mice treated with SNPs; no adverse effects were recorded following SNP application. SNPs are unable to penetrate the skin barrier and no detrimental effects on keratinocytes have been reported after application [41]; therefore, SNPs also have potential utility as a safe preservative in cosmetic.

CONCLUSIONS

This study investigated optimal conditions for SNP biosynthesis from *M. aquatica* L. var. *aquatica* leaf extract. Wound healing and bactericidal activity against *P. aeruginosa* and *S. aureus* were also evaluated. Nanoparticles were characterized by UV–Vis, SEM, TEM, DLS, and FTIR. Optimal conditions for SNP synthesis were 5 mM $AgNO_3$, 40 mg/ml initial *M. aquatica* L. var. *aquatica* leaf extract, and a reaction time of 1 h. SNPs had an average size of 65.62 nm and an irregular spherical shape. SNPs inhibited the growth of *P. aeruginosa* and *S. aureus*; antibacterial effect was dose dependent. SNPs accelerated the wound healing process with no effect on weight gain in mice. These findings support the use of SNPs in the treatment of burn wounds. Further studies are recommended to investigate the mechanisms of wound healing by SNPs biosynthesized from *M. aquatica* L. var. *aquatica* leaf extract.

LIST OF ABBREVIATION

DLS: Dynamic light scattering
FTIR: Fourier transform infrared spectroscopy
SEM: Scanning electron microscopy
SNPs: Silver nanoparticles
SPRs: Surface plasmon resonances
TEM: Transmission electron microscopy
Uv-Vis: Ultraviolet-visible

COMPETING INTERESTS

There are no competing interest for any of the authors.

AUTHORS' CONTRIBUTIONS

Author's additions needed.

ACKNOWLEDGEMENTS

Author's additions needed.

REFERENCES

1. Alharbi NS, Alsubhi NS, Felimban AI. Green synthesis of silver nanoparticles using medicinal plants: characterization and application. J Radiat Res Appl Sci. 2022;15(3):109–24. Available from: https://doi.org/10.1016/j.jrras.2022.06.012.
2. Akhtar MF, Irshad M, Ali S, Summer M, Jawad M, Akhter MF, et al. Spectrophotometric, microscopic, crystallographic and X-ray based optimization and biological applications of Olea paniculata leaf extract mediated silver nanoparticles. S Afr J Bot. 2024;166:97–105. Available from: https://doi.org/10.1016/j.sajb.2024.01.019.
3. Shahcheraghi N, Golchin H, Sadri Z, Tabari Y, Borhanifar F, Makani S. Nano-Biotechnology, an Applicable Approach for Sustainable Future. Biotech. 2022;12(3). Available from: https://doi.org/10.1007/s13205-021-03108-9.
4. Nyabadza A, McCarthy E, Makhesana M, Heidarinassab S, Plouze A, Vazquez M, et al. A review of physical, chemical and biological synthesis methods of bimetallic nanoparticles and applications in sensing, water treatment, biomedicine, catalysis and hydrogen storage. Adv Colloid Interface Sci. 2023;321. Available from: https://doi.org/10.1016/j.cis.2023.103010.
5. Rani N, Singh P, Kumar S, Kumar P, Bhankar V, Kumar K. Plant-Mediated Synthesis of Nanoparticles and Their Applications: A Review. Mater Res Bull. 2023;163. Available from: https://doi.org/10.1016/j.materresbull.2023.112233.
6. Magdum AB, Waghmode RS, Shinde KV, Mane MP, Kamble MV, Kamble RS, et al. Biogenic synthesis of silver nanoparticles from leaves extract of Decaschistia trilobata an endemic shrub and its application as antioxidant, antibacterial, anti-inflammatory and dye reduction. Catal Commun. 2024;187. Available from: https://doi.org/10.1016/j.catcom.2024.106865.
7. Haleem A, Javaid M, Singh RP, Rab S, Suman R. Applications of Nanotechnology in Medical Field: A Brief Review. Glob Health J. 2023;7(2):70–7. Available from: https://doi.org/10.1016/j.glohj.2023.02.008.
8. Abbasi R, Shineh G, Mobaraki M, Doughty S, Tayebi L. Structural parameters of nanoparticles affecting their toxicity for biomedical applications: a review. J Nanopart Res. 2023;25(3):43. Available from: https://doi.org/10.1007/s11051-023-05690-w.
9. Bhattacharjee R, Negi A, Bhattacharya B, Dey T, Mitra P, Preetam S, et al. Nanotheranostics to Target Antibiotic-Resistant Bacteria: strategies and Applications. OpenNano. 2023;11. Available from: https://doi.org/10.1016/j.onano.2023.100138.
10. Uddin TM, Chakraborty AJ, Khusro A, Zidan BR, Mitra S, Emran TB, et al. Antibiotic resistance in microbes: History, mechanisms, therapeutic strategies and future prospects. J Infect Public Health. 2021;14(12):1750–66. Available from: https://doi.org/10.1016/j.jiph.2021.10.020.
11. Jeong SH, Yeo SY, Yi SC. The Effect of Filler Particle Size on the Antibacterial Properties of Compounded Poly-mer/Silver Fibers. Journal of Materials Science. 2005;Available from: https://doi.org/10.1007/s10853-005-4339-8.
12. Mukaratirwa-Muchanyereyi N, Gusha C, Mujuru M, Guyo U, Nyoni S. Synthesis of silver nanoparticles using plant extracts from Erythrina abyssinica aerial parts and assessment of their anti-bacterial and anti-oxidant activities. Results Chem. 2022;4. Available from: https://doi.org/10.1016/j.rechem.2022.100402.
13. Giri AK, Jena B, Biswal B, Pradhan AK, Arakha M, Acharya S, et al. Green synthesis and characterization of silver nanoparticles using Eugenia roxburghii DC. extract and activity against biofilm-producing bacteria. Sci Rep. 2022;12(1):8383. Available from: https://doi.org/10.1038/s41598-022-12484-y.
14. Ohiduzzaman M, Khan MN, Khan KA, Paul B. Biosynthesis of silver nanoparticles by banana pulp extract: Characterizations, antibacterial activity, and bioelectricity generation. Heliyon. 2024;10(3). Available from: https://doi.org/10.1016/j.heliyon.2024.e25520.
15. Gabriela AM, Gabriela MO, Luis AM, Reinaldo PR, Michael HM, Rodolfo GP, et al. Biosynthesis of Silver Nanoparticles Using Mint Leaf Extract (Mentha piperita) and Their Antibacterial Activity. Adv Sci Eng Med. 2017;9(11):914–23. Available from: https://doi.org/10.1166/asem.2017.2076.
16. Hasan KM, Xiaoyi L, Shaoqin Z, Horváth PG, Bak M, Bejó L, et al. Functional silver nanoparticles synthesis from sustainable point of view: 2000 to 2023 % UNKNOWN UNICODE CHARACTER 02012 (FIGURE DASH) A review on game changing materials. Heliyon. 2022;8(12). Available from: https://doi.org/10.1016/j.heliyon.2022.e12322.

17. Donga S, Chanda S. Facile green synthesis of silver nanoparticles using Mangifera indica seed aqueous extract and its antimicrobial, antioxidant and cytotoxic potential (3-in-1 system). Artif Cells Nanomed Biotechnol. 2021;49(1):292–302. Available from: https://doi.org/10.1080/21691401.2021.1899193.
18. Abdallah BM, Ali EM. Green Synthesis of Silver Nanoparticles Using the Lotus lalambensis Aqueous Leaf Extract and Their Anti-Candidal Activity against Oral Candidiasis. ACS Omega. 2021;6(12):8151–62. Available from: https://doi.org/10.1021/acsomega.0c06009.
19. Varadavenkatesan T, Selvaraj R, Vinayagam R. Phyto-synthesis of silver nanoparticles from Mussaenda erythrophylla leaf extract and their application in catalytic degradation of methyl orange dye. J Mol Liq. 2016;221:1063–70. Available from: https://doi.org/10.1016/j.molliq.2016.06.064.
20. Ross BM, Tasoglu S, Lee LP. Plasmon Resonance Differences between the Near- and Far-Field and Implications for Molecular Detection. Plasmonics: Metallic Nanostructures and Their Optical Properties VII. 2009;Available from: https://doi.org/10.1117/12.826804.
21. Gupta P, Ramrakhiani M. Influence of the Particle Size on the Optical Properties of CdSe Nanoparticles. Open Nanosci J. 2009;3(1):15–9. Available from: https://doi.org/10.2174/1874140100903010015.
22. Sharma V, Javed B, Estrada G, Byrne HJ, Tian F. In situ tuning and investigating the growth process of size controllable gold nanoparticles and statistical size prediction analysis. Colloids Surf A Physicochem Eng Asp. 2024;681. Available from: https://doi.org/10.1016/j.colsurfa.2023.132733.
23. Karade VC, Dongale TD, Sahoo SC, Kollu P, Chougale AD, Patil PS, et al. Effect of reaction time on structural and magnetic properties of green-synthesized magnetic nanoparticles. J Phys Chem Solids. 2018;120:161–6. Available from: https://doi.org/10.1016/j.jpcs.2018.04.040.
24. Wang Y, Li S, Ren X, Yu S, Meng X. Nano-engineering nanomedicines with customized functions for tumor treatment applications. J Nanobiotechnology. 2023;21(1):250. Available from: https://doi.org/10.1186/s12951-023-01975-3.
25. Orgen SB, Balela MD. Effect of Reaction Time on the Morphology of CuO Nanostructured Electrode for Pseudocapacitor Application. Conference Series; 2021. Available from: https://doi.org/10.1088/1742-6596/1974/1/012006.
26. Amara YT, Beldjilali M, Kermezli FZ, Chikhi I, Taha I, Ismail I, et al. Mentha aquatica leaf extract mediated phytosynthesis of silver nanoparticles: antioxidant, catalytic and anti-microbial activity. New J Chem. 2023;47(29):13841–54. Available from: https://doi.org/10.1039/d3nj01737k.
27. Khalil S, Mehmood A, Khan MAR, Ahmad KS, Abasi F, Raffi M, et al. Antibacterial, antioxidant and photocatalytic activity of novel Rubus ellipticus leaf mediated silver nanoparticles. J Saudi Chem Soc. 2023;27(1). Available from: https://doi.org/10.1016/j.jscs.2022.101576.
28. Mapara N, Sharma M, Shriram V, Bharadwaj R, Mohite KC, Kumar V. Antimicrobial potentials of Helicteres isora silver nanoparticles against extensively drug-resistant (XDR) clinical isolates of Pseudomonas aeruginosa. Appl Microbiol Biotechnol. 2015;99(24):10655–67. Available from: https://doi.org/10.1007/s00253-015-6938-x.
29. Orlov IA, Sankova TP, Babich PS, Sosnin IM, Ilyechova EY, Kirilenko DA, et al. New silver nanoparticles induce apoptosis-like process in E. coli and interfere with mammalian copper metabolism. Int J Nanomedicine. 2016;11:6561–74. Available from: https://doi.org/10.2147/IJN.S117745.
30. Mohanty S, Mishra S, Jena P, Jacob B, Sarkar B, Sonawane A. An investigation on the antibacterial, cytotoxic, and antibiofilm efficacy of starch-stabilized silver nanoparticles. Nanomedicine. 2012;8(6):916–24. Available from: https://doi.org/10.1016/j.nano.2011.11.007.
31. Jiang B, Larson JC, Drapala PW, Pérez-Luna VH, Kang-Mieler JJ, Brey EM. Investigation of lysine acrylate containing poly(N-isopropylacrylamide) hydrogels as wound dressings in normal and infected wounds. J Biomed Mater Res - Part B Appl Biomater. 2012;100B(3). Available from: https://doi.org/10.1002/jbm.b.31991.
32. Huang Z, Zheng X, Yan D, Yin G, Liao X, Kang Y, et al. Toxicological effect of ZnO nanoparticles based on bacteria. Langmuir. 2008;24(8):4140–4. Available from: https://doi.org/10.1021/la7035949.
33. Pal S, Tak YK, Song JM. Does the antibacterial activity of silver nanoparticles depend on the shape of the nanoparticle? A study of the gram-negative bacterium Escherichia coli. J Biol Chem. 2015;•••. Available from: https://doi.org/10.1128/AEM.02218-06.
34. Hamida RS, Ali MA, Goda DA, Khalil MI, Al-Zaban MI. Novel Biogenic Silver Nanoparticle-Induced Reactive Oxygen Species Inhibit the Biofilm Formation and Virulence Activities of Methicillin-Resistant Staphylococcus aureus (MRSA) Strain. Front Bioeng Biotechnol. 2020;8:433. Available from: https://doi.org/10.3389/fbioe.2020.00433.
35. Viljoen A, Foster SJ, Fantner GE, Hobbs JK, Dufrêne YF. Scratching the Surface: Bacterial Cell Envelopes at the Nanoscale. MBio. 2020;11(1). Available from: https://doi.org/10.1128/mBio.03020-19.
36. Gurunathan S, Han JW, Kwon DN, Kim JH. Enhanced antibacterial and anti-biofilm activities of silver nanoparticles against Gram-negative and Gram-positive bacteria. Nanoscale Res Lett. 2014;9(1):373. Available from: https://doi.org/10.1186/1556-276X-9-373.
37. Gouyau J, Duval RE, Boudier A, Lamouroux E. Investigation of nanoparticle metallic core antibacterial activity: gold and silver nanoparticles against Escherichia coli and staphylococcus aureus. Int J Mol Sci. 2021;22(4):1905. Available from: https://doi.org/10.3390/ijms22041905.
38. Das P, Majumder R, Sen N, Nandi SK, Ghosh A, Mandal M, et al. A computational analysis to evaluate deleterious SNPs of GSK3β, a multifunctional and regulatory protein, for metabolism, wound healing, and migratory processes. Int J Biol Macromol. 2024;256(Pt 1). Available from: https://doi.org/10.1016/j.ijbiomac.2023.128262.
39. Qin W, Wu Y, Liu J, Yuan X, Gao J. A Comprehensive Review of the Application of Nanoparticles in Diabetic Wound Healing: Therapeutic Potential and Future Perspectives. Int J Nanomedicine. 2022;17:6007–29. Available from: https://doi.org/10.2147/IJN.S386585.
40. Lakkim V, Reddy MC, Lekkala VV, Lebaka VR, Korivi M, Lomada D. Antioxidant Efficacy of Green-Synthesized Silver Nanoparticles Promotes Wound Healing in Mice. Pharmaceutics. 2023;15(5):1517. Available from: https://doi.org/10.3390/pharmaceutics15051517.
41. Gupta V, Mohapatra S, Mishra H, Farooq U, Kumar K, Ansari MJ, et al. Nanotechnology in Cosmetics and Cosmeceuticals-A Review of Latest Advancements. Gels. 2022;8(3):173. Available from: https://doi.org/10.3390/gels8030173.